



Contents lists available at CEPM

Computational Engineering and Physical Modeling

Journal homepage: www.jcepm.com



Numerical Analysis of Flow and Heat Transfer Characteristics between Two Parallel Plates with Constriction(s)

I. Rahman*, M.A. Shahriar, S. Rahman

Department of Mechanical Engineering, Military Institute of Science and Technology, Dhaka, Bangladesh

Corresponding author: ishtier.rahman@gmail.com

 <https://doi.org/10.22115/CEPM.2021.281818.1167>

ARTICLE INFO

Article history:

Received: 18 April 2021

Revised: 09 August 2021

Accepted: 10 August 2021

Keywords:

Numerical;

CFD;

Restriction;

Reynolds number;

Pressure;

Velocity.

ABSTRACT

A numerical study involving graphical analysis has been carried out to investigate fluid flow and heat transfer between two stationary horizontal plates possessing blocks (which restricts flow). Important parameters corresponding to pressure, velocity, temperature, heat transfer coefficient and Nusselt Number have been under the spotlight. Multiple investigations have been undertaken to observe the flow and heat transfer characteristics not only by altering the size of blocks but also by changing the number of blocks. As the blocks reduce the area of flow, following the Continuity equation, reduction of flow area increases the flow velocity and makes the flow turbulent. And the rise of fluid velocity lowers the pressure according to Bernoulli's principle. Moreover, the presence of blocks creates recirculation of fluid which increases the available time for heat gaining while heat flux is being applied. Blocks contribute to the increase in temperature of the fluid. The higher velocity of fluid causes higher collision among fluid particles. Thus, the heat transfer coefficient and Nusselt Number increase.

How to cite this article: Rahman, I., Shahriar, M. A., & Rahman, S. (2021). Numerical Analysis of Flow and Heat Transfer Characteristics between Two Parallel Plates with Constriction(s). *Computational Engineering and Physical Modeling*, 4(3), 55–69. <https://doi.org/10.22115/cepm.2021.281818.1167>

2588-6959/ © 2021 The Authors. Published by Pouyan Press.

This is an open access article under the CC BY license (<http://creativecommons.org/licenses/by/4.0/>).



1. Introduction

The fluid flow through the parallel plate channel experiences changes in pressure. The pressure drop is the main concern, as the fluid is passed through parallel channels. The wall pressure is decreased as the length of the surface is increased along the horizontal axis. This effect is enhanced by the presence of small restrictions in the fluid passage [1]. This study incorporates the effect of restrictions placed on the parallel flow of the fluid. The blocks serve as a constraint to the flow, as the pressure decreases sharply. Linear pressure drop takes place based on the effects of the blocks. If the effect of these blocks is derelict the linear pressure drop takes place. Due to the viscosity effect, the wall pressure is not recovered fully in downstream, these losses are irrecoverable. This study shows that as the length of the restriction is increased these losses are also increased. The ratio of irreversible losses has increased exponentially with the length. On the contrary, these losses are minor if the length of the restriction is small.

The analysis is based upon the Poiseuille flow, which is a pressure-driven flow. This is considered a swirl-free flow with axisymmetric properties. The pressure varies in the x-direction and flow is essentially axial ($u \neq 0, v = w = 0$) [2]. The flow is considered far downstream so that it is developed to some extent and the effect of wall shear is diminished. This is done to perform profile analysis of the fluid between two parallel plates of infinite length.

The velocity profile of the fluid is also discussed as the restriction leads to the acceleration of the fluid, the nonlinear behavior is noticed. Due to the flow separation in the flow, the velocity is increased. This increment in velocity leads to the pressure drop in the channel. The pressure drop has adverse consequences as it can cause the collapse of the channel. To control the flow, velocity profile analysis is imperative. However, the velocity profile is parabolic for Poiseuille flow with zero velocity at the top and bottom plate with maximum velocity in the center line.

The third parameter to be studied is heat transfer. These restrictions in the flow of the fluid lead to varying heat transfer. The blocks lead to recirculation of the fluid in the channel, which may aid in the increase of heat transfer. The behavior of these characteristics is shown numerically by taking surface heat flux constant using the mathematical model.

Perseverance of this research is to analyze the effect of restriction on the flow channel as well as measure the pressure of water at the upper and lower plate. Also the measurement of pressure and velocity along the conveniently chosen line between plates is performed. Moreover, calculate Nusselt Number and Convective heat transfer coefficient at the outlet were also the goal.

This research will prove to be advantageous in designing plates or heat exchangers, as the selection of wavy plates provides energy saving. Along with this, the research depicts the idea of restriction in blood vessels in the form of fats. This causes the pressure drop and velocity changes in blood vessels.

2. Literature review

To analyze the heat transfer and pressure drop in corrugated channels and smooth pipes Sunden and Skoldheden [3,4] developed an experimental setup at constant heat flux and validated it with numerical methods. As the research on heat transfer was carried on, the effect of three-dimensional hydrodynamics on heat transfer enhancement in corrugated channels was studied [5]. Newtonian and Non-Newtonian fluids flowing in corrugated channels had different heat transfer properties [6]. Fabbri [7,8] investigated laminar convective heat transfer in a channel with smooth and corrugated walls. The change in the angle of the corrugated plane also affected the heat transfer. It was depicted by using the same APV SR3 plates with different angles [9]. To observe adiabatic concurrent gas and liquid interaction in horizontal corrugated channel Gradeck and Lebouche used nitrogen and water as a working fluid [10]. Zimmerer et al. [11] found that the angle of inclination and wavelength of corrugated flow had various effects of heat and mass transfer in a heat exchanger. To determine the heat transfer rates, Wang and Chen [12] implemented a simple and effective technique of coordinate transformation and the spline alternating-direction implicit method. Effects of wavy geometry, number of Reynolds, and number of Prandtl on skin friction and number of Nusselt were taken into contemplation. Hamza et al. [13] experimentally studied the effects of the operating parameters on laminar flow forced-convection heat transfer in channel with V upper plate and gas as operating fluid. Metwally and Manglik [14] simulated laminar periodically created forced convection in sinusoidal corrugated-plate channels using the finite-difference control volume technique. Islamoglu and Parmaksizoglu [15–17] explored numerically and experimentally the impact of channel height on enhancing heat transfer behavior in a corrugated heat exchanger channel. Furthermore, artificial networks were used to evaluate the heat transfer in corrugated channels. Naphon [18–20] analyzed the heat transfer and pressure fall characteristics of a corrugated channel with various V-shaped wavy plates and channel heights. Heat transfer can be increased by increasing turbulence in the fluid by adding some pattern in the plates. Moreover, the usage of Nanofluids as a coolant of the plate has increased heat flux [21]. Analyzing the effect of boundary conditions on conjugate heat transfer in parallel micro sink resulted that at constant heat flux boundary conditions the mean temperature of the fluid and solid decreases. On the other hand, constant temperature boundary conditions adverse results were shown in the CFD model [22]. The effect of the number of plates and distance between plates was found by CFD analysis of moment and heat transfer non-Newtonian fluids in the plate heat exchanger. This deduced that heat transfer does not depend upon the number or distance of plates rather it depends upon pumping power [23]. Furthermore, the mathematical equation was developed to analyze the effect of maldistribution in parallel plate-fine heat exchanger. The three configurations which were assessed were conventional header configurations, a punched baffle header configuration and a quasi-S header configuration, respectively. This also stated that the effect of maldistribution can be described by applying good synergy flow of hot and cold fluid in adjacent heat exchanger [24]. For the heat transfer enhancement in tubes, optimization of the tube design and insertion of porous material was done using a genetic algorithm along with CFD analysis. This stated that the

porous inserts in tube enhanced heat transfer [25]. The heat transfer for the parallel plate at constant temperature conditions was investigated by the DPD method. It was found that Yaghoubi and fan weight function controlled the velocity and temperature fluctuation near-wall very well. It was a novel method and showed better results rather than the classic one [26].

3. Methodology

For the analysis, 2D geometry was generated using ANSYS. The Fig. 1 shows the geometric model, along with the dimensions. The two domains were performed first with single restriction and the other with multiple restrictions. In pre-processing, the fine mesh was generated on the model to reduce computational effort. Square meshing was performed for the flow channel. The solution was evaluated and the skewness of the mesh was reduced by introducing smoothness function (Fig. 2).

Water was used as fluid and Aluminum was selected as plate material. For the turbulent flow analysis, K-epsilon equation was selected and the energy equation was activated. Surface body was as water-liquid in Cell Zone for precise heat transfer.

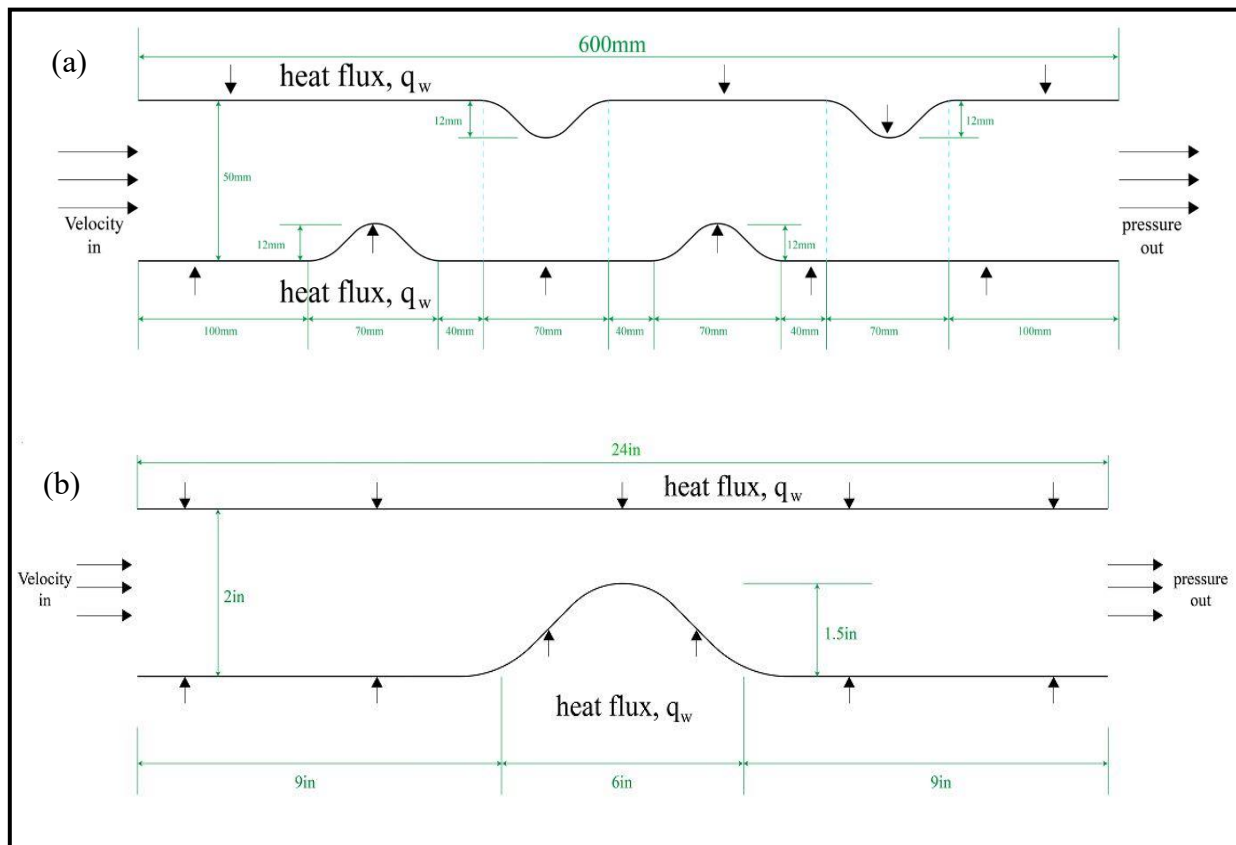


Fig. 1. Computational Model (a) Single Restriction (b) Multiple Restriction.

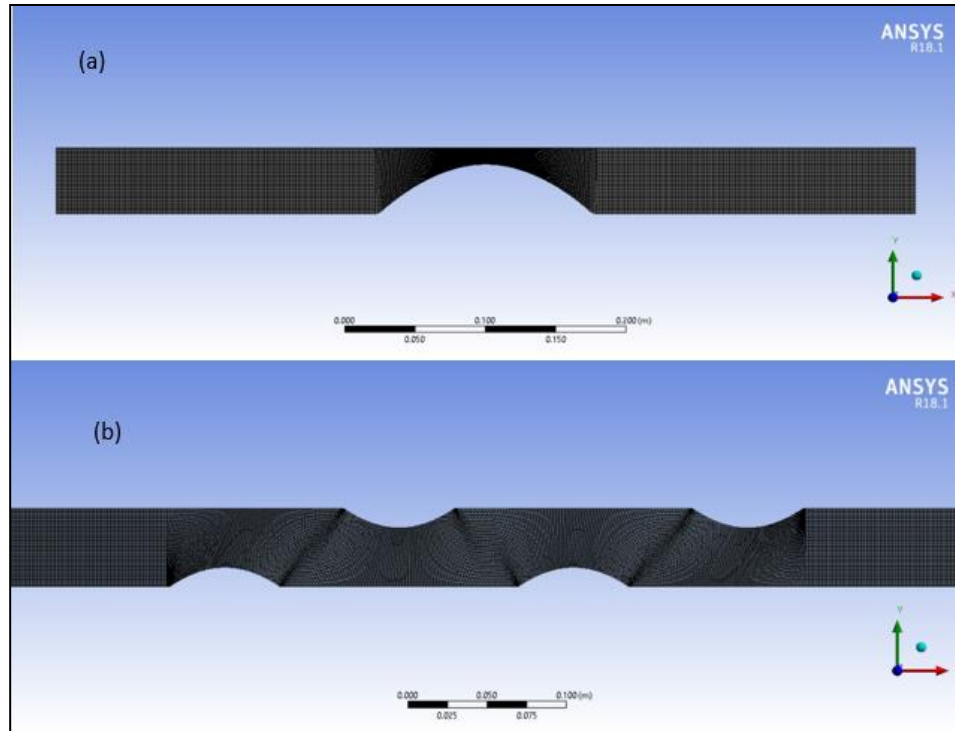


Fig. 2. Meshing (a) Single restriction (b) Multiple Restriction.

Some reference values were specified for starting the computation from the inlet. As the density was kept constant, the flow was incompressible. No pressure was applied in the inlet and temperature was specified. Turbulence intensity $I = \sqrt{\frac{2}{3}} k/u$, is also specified at the inlet for calculations. For outlet conditions, gauge pressure is assumed to be constant. A radial equilibrium pressure distribution option is available for cases where that is not appropriate, e.g. for strongly swirling flows. Symmetric boundary conditions are advantages when analyzing pipes or other flow channels. After specifying boundary conditions, the analysis was performed. Number of iterations is specified as 1000, according to the convergence of the solution. To view the results and evaluate the behavior of flow by varying some properties, the post-CFD module is utilized.

4. Governing equations

The fluid flow analysis is governed by Navier Stokes Equation. It is based on the conservation of momentum with gravity, pressure and shear forces [27].

$$\rho a + \rho g = -\nabla p + \mu \nabla^2 V \quad (1)$$

Eq. 1 gives the acceleration of the fluid. Here ‘a’ represents Lagrangian acceleration and ‘g’ is the gravitational acceleration. This equation is further simplified for the shear stress gradient. For laminar flow in the horizontal direction, the Eq. 2 was derived from Eq. 1 by applied zero acceleration conditions.

$$\frac{y^2}{2} \cdot \frac{dp}{dx} + Ay + B = \mu u \quad (2)$$

'y' is the vertical plan direction and 'u' is the horizontal velocity of the fluid. 'A' and 'B' are the boundary conditions that are to be found. For infinite, horizontal channel and specific boundary conditions, the Eq. 2 is further simplified and T is found to be:

$$T = \left(y - \frac{a}{2}\right) \frac{dp}{dx} \quad (3)$$

Considering the flow to be laminar, the discharge flow is given in Eq 4. The partial derivative equation depicts the change in the pressure along with the fluid flow. The variation of the velocity profile is given in Eq. 4.

$$\mu \left(\frac{d^2u}{dy^2}\right) = \rho g_x + \frac{dp}{dx} \quad (4)$$

These equations utilize the Continuity equation and Bernoulli's equation to provide a complete solution to the stated problem.

5. Results and discussion

5.1. Computational domain-I

For the computational domain as given in Fig. 1(a), the stationary parallel plates are separated from a fixed distance. The fluid enters from the left side, and leaves from the right side. Heat flux is applied longitudinally to both upper and lower plates to heat the water. Moreover, the middle zone of the lower plate is pressed from outside in such a way that a sinusoidal region is created inside.

5.1.1. Effect of pressure

In Fig. 3, it is seen that there is a slight decrement in pressure due to the wall friction. As the fluid reaches the restriction zone, there is an abrupt decrease in the pressure. Because the block lessens the flow area causes an increase in flow speed to keep the flow rate constant. Pressure drop increases with increasing Reynolds Number. The pressure drop across the lower plate is the highest. As the constriction seizes pressure tends to increase but never reaches its initial value as the loss is irrecoverable due to viscous effect.

5.1.2. Effect of velocity

From Fig. 5 it is depicted that there is slight increase in the velocity at the entrance due to a slight pressure drop. Since the arrangement parallel plates are kept horizontal, gravity does not affect. So, the pressure difference between the two sections drives the flow while the viscous effects provide a restraining force that exactly balances the pressure forces. The fluid moves with constant velocity. As the restriction height is increased, the flow area is reduced, this escalates the velocity of the fluid. Fig. 5 shows the variation of velocity with Reynold number.

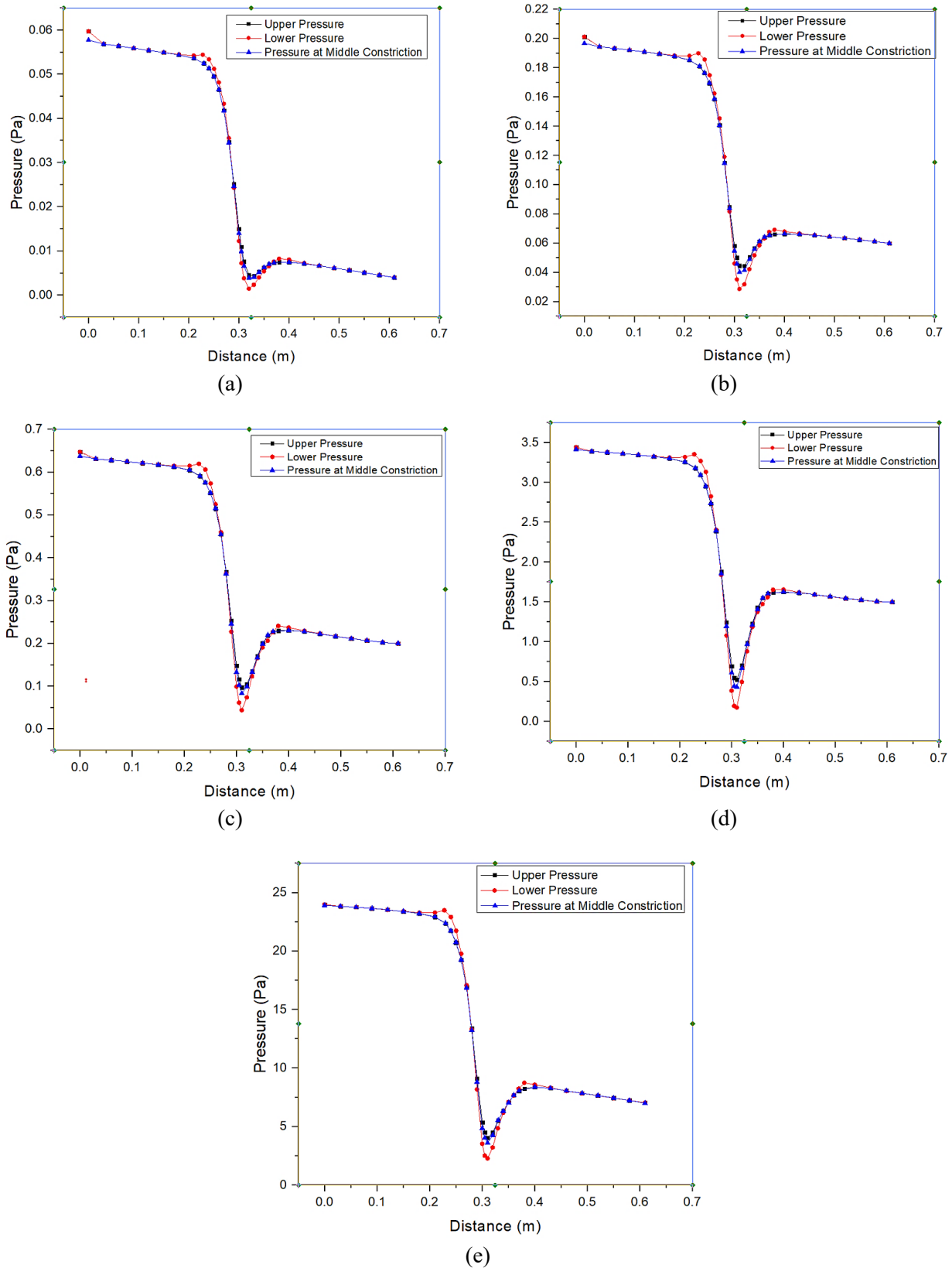


Fig. 3. Effect of fluid flow on Pressure (a) $Re=100$ (b) $Re=200$ (c) $Re=400$ (d) $Re=1000$ (e) $Re=2500$.

5.1.3. Effect of outlet temperature

At the time of flow, heat flux is applied from outside to both walls. If Reynolds Number is low, fluid velocity will also be low. So, fluid will get more time to absorb heat from the walls. Thereby the temperature of the fluid will increase rapidly. This variation is shown in Fig. 4(a). If the Reynold number is high the temperature gain will be low. Moreover, the temperature of the fluid close to both upper and lower walls will be more than the fluid at the centerline because heat flux is applied to the walls. Owing to the presence of blocks, there will be recirculation of water that creates turbulence. Due to this, water tends to stay in one place sometimes. Thus more heat gaining is possible. Although outlet temperature falls as Reynolds Number increases once a higher Reynolds Number is reached, temperature no longer falls rather becomes almost constant as shown in Fig. 4(b).

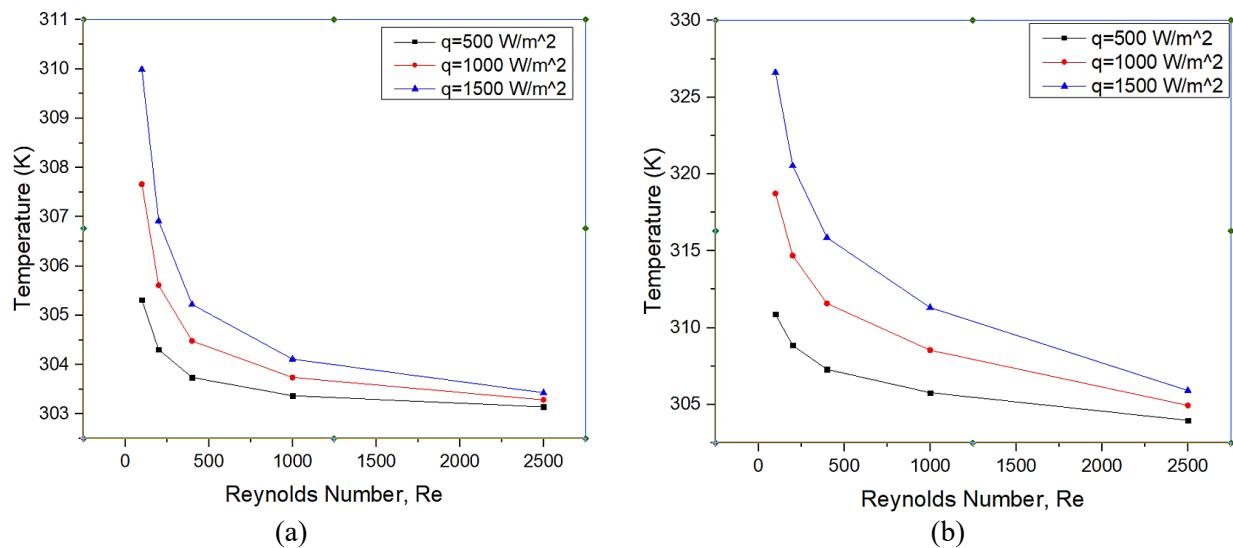


Fig. 4. Variation of (a) outlet stream temp (b) outlet wall temperature with Reynolds Number.

5.1.4. Effect of nusselt number and heat transfer co-efficient

The flow inside the setup is turbulent because of the rapid rise of velocity and there is substantial breaking away from the tube wall and condition is described as turbulent flow with significant mixing of the boundary layer and the bulk fluid. Due to higher collision among fluid particles, heat transition rate increases. So, theoretically, there should be an increase of heat transfer coefficient with increasing Reynolds Number which can be observed in Fig. 6(a).

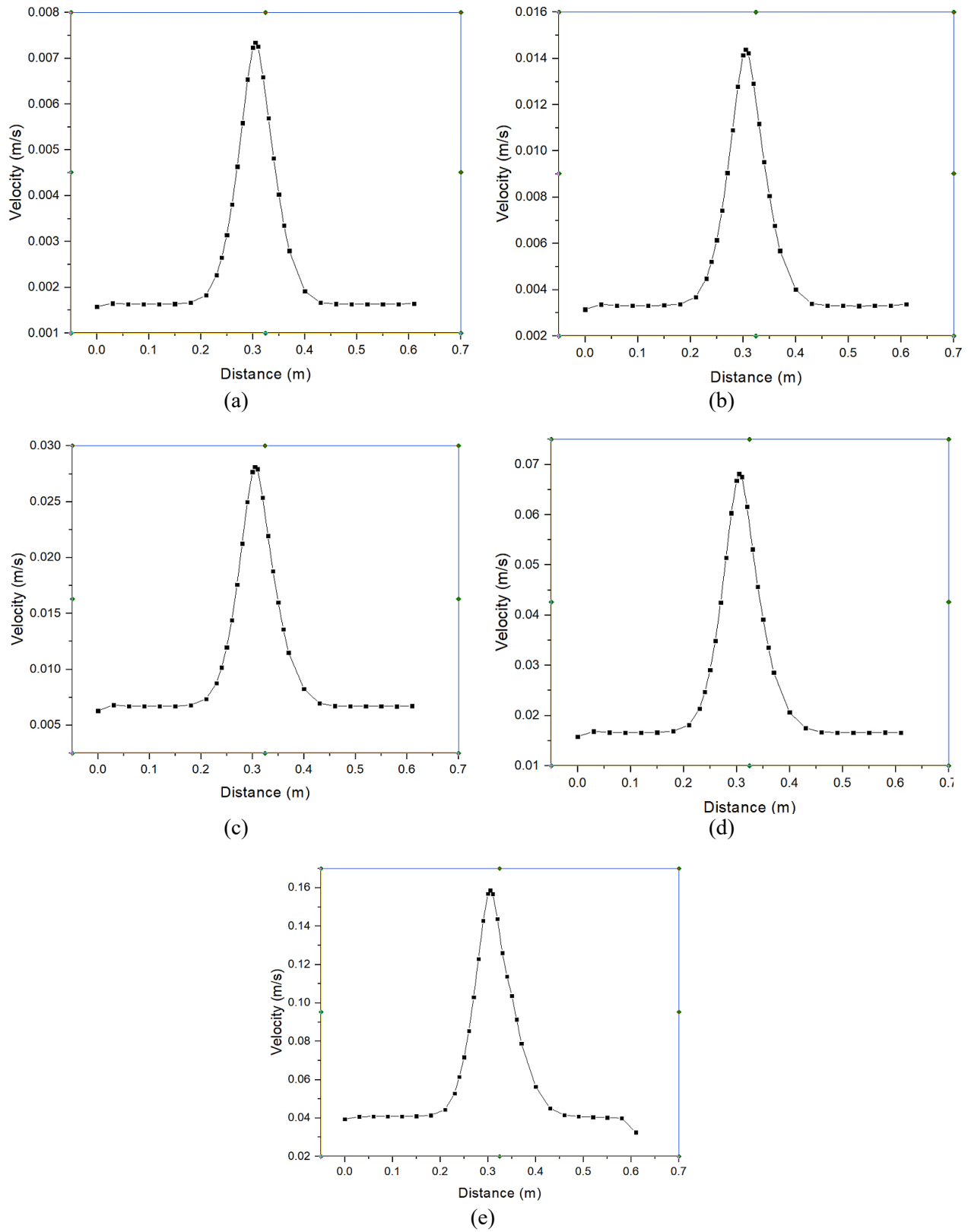


Fig. 5. Variation of velocity with Reynold Number (a) $Re=100$ (b) $Re=200$ (c) $Re=400$ (d) $Re=1000$ (e) $Re= 2500$.

So, the heat transfer coefficient increases with the Reynolds Number for wavy channel configuration. The size or amplitude of wavy blocks has a significant influence on the growth of recirculation zones promoting the mixing of fluid in the thermal boundary layer. Thus, the convective heat transfer coefficient is enhanced.

With the increase of heat transfer coefficient, Nusselt Number also increases as Nusselt Number is the function of heat transfer co-efficient which is shown in Fig. 6(b).

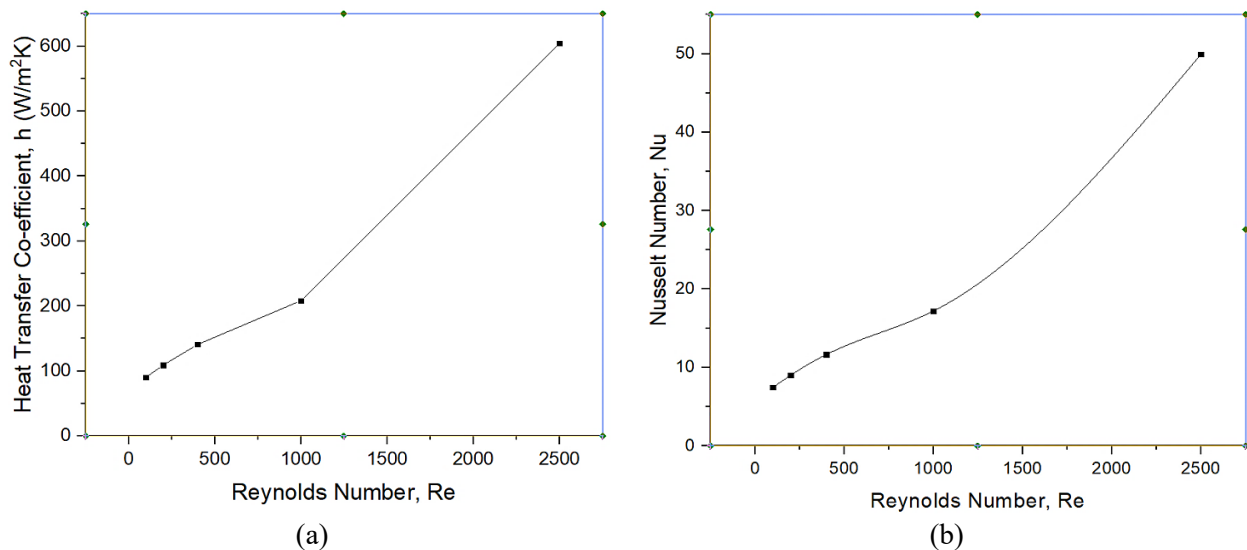


Fig. 6. Variation of (a) Heat transfer Co-efficient (b) Nusselt Number with Reynold Number.

5.2. Computational domain II

For this domain, better results are expected as the first setup contains one block only while this one contains four blocks. However, the size or amplitude of the constriction is an important factor too and the block of setup-I has a much higher amplitude and size than each block of setup-II. So both the setups contribute to escalating flow velocity, pressure drop, and heat transfer coefficient. In this setup, four blocks are constructed instead of one as shown in Figure 1(b). Each block is of the same dimension and is smaller than the block of the first setup.

5.2.1. Effect of pressure

In Fig. 9, the initial wall pressure falls as it tends to coincide with the middle pressure. The maximum pressure drop occurs at the lower plate for first and third constriction; at the upper plate for second and fourth constriction. There is an overall decrease of pressure for each of the four constrictions. Furthermore, magnitude of pressure drop increases with increasing Reynolds Number.

5.2.2. Effect of velocity

Similar nature of velocity fluctuation in the multi-restriction channel is observed as found in setup-I shown in Fig. 10.

5.2.3. Effect of outlet as the temperature

The effect of outlet temperature for the multi-restriction channel is shown in Fig. 7. It shows similar behavior like setup-I.

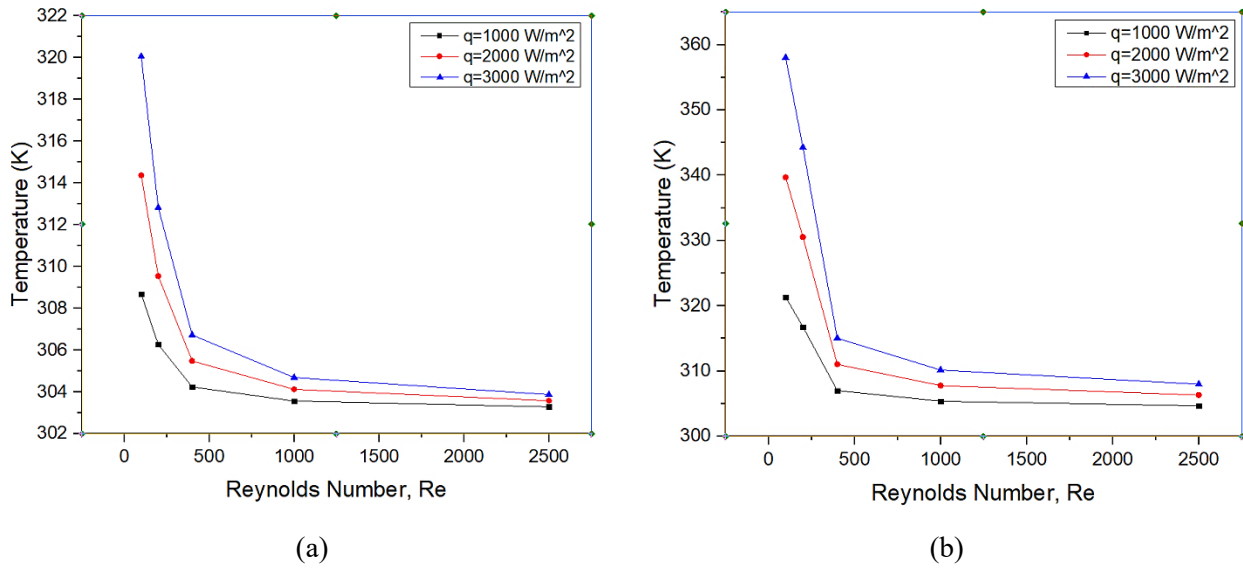


Fig. 7. Variation of (a) outlet stream temp (b) outlet wall temperature with Reynolds Number.

5.2.4. Effect of Nusselt Number and Heat Transfer Co-efficient

The same effect is assessed for the Nusselt number and heat transfer coefficient for setup-II as in the single restriction channel in Fig. 8. The slight variation is the rapid increase of both heat transfer coefficient and Nusselt Number which is due to multiple restrictions.

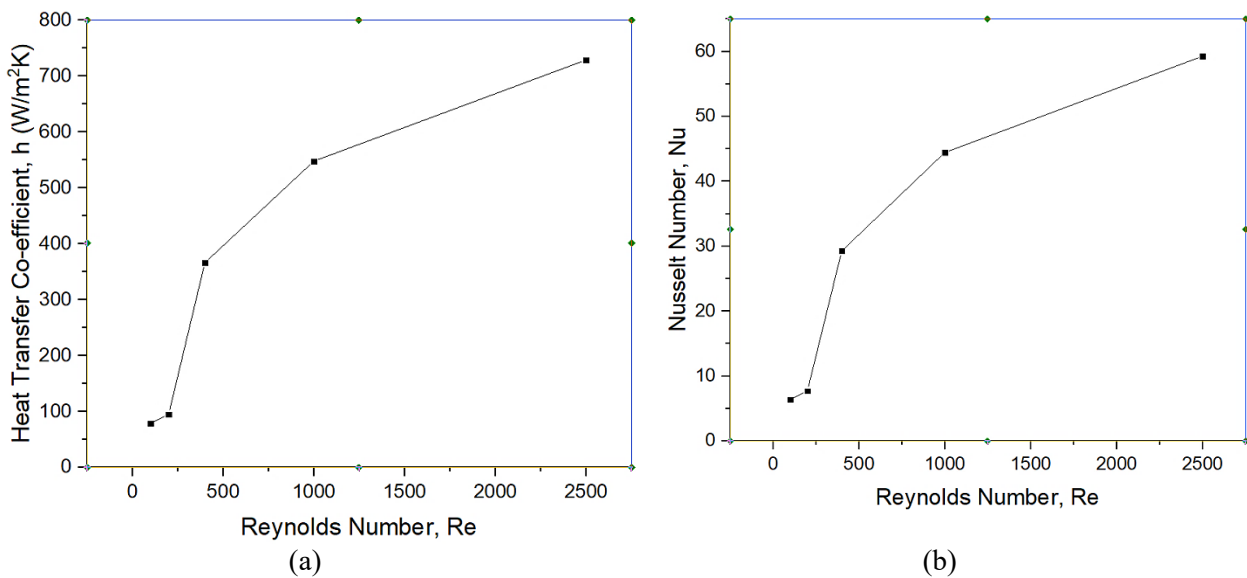


Fig. 8. Effect of (a) Heat transfer Co-efficient and (b) Nusselt Number in Multi-restriction flow.

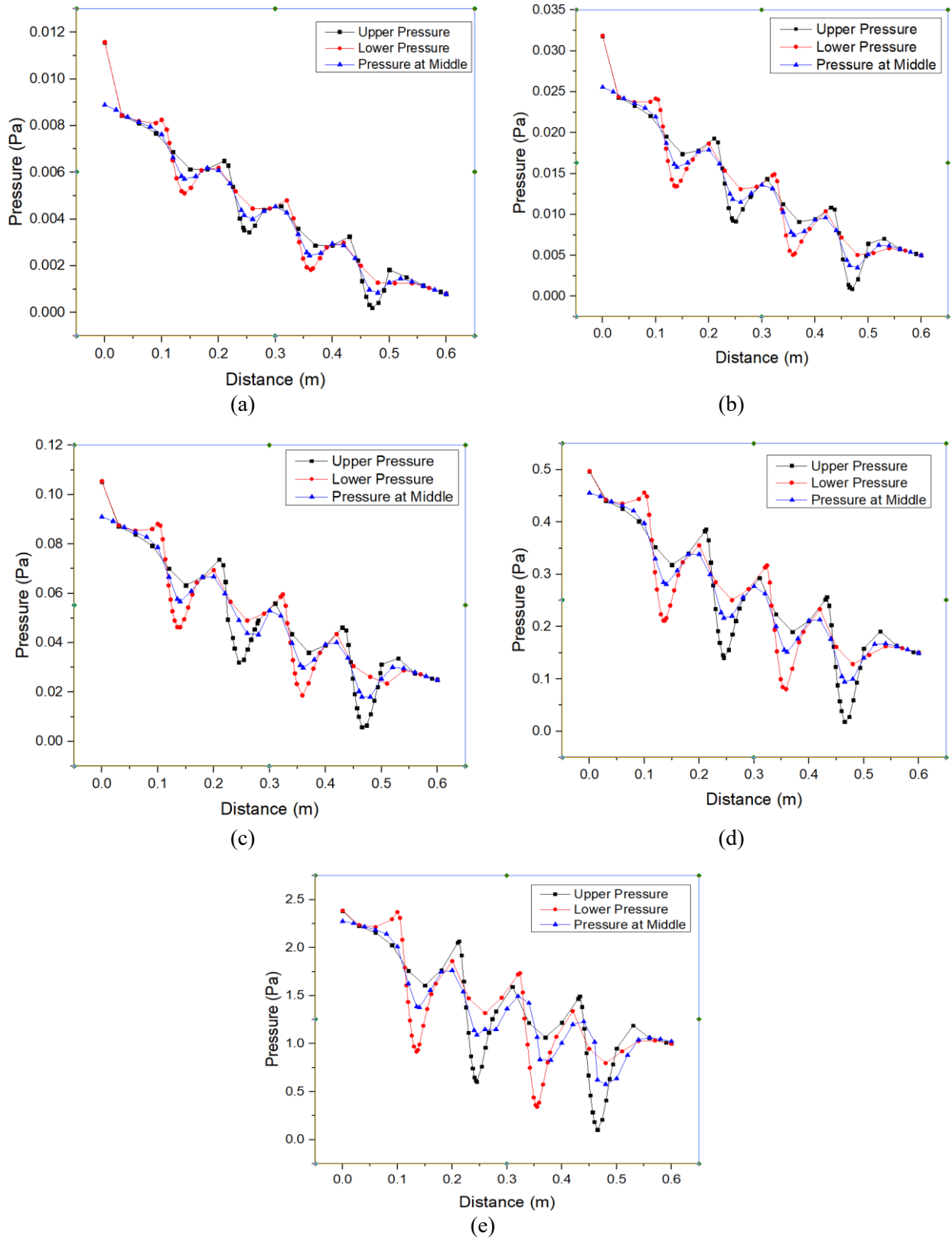


Fig. 9. Effect of fluid flow on velocity Multi-restriction (a) $Re=100$ (b) $Re=200$ (c) $Re=400$ (d) $Re=1000$ (e) $Re=2500$.

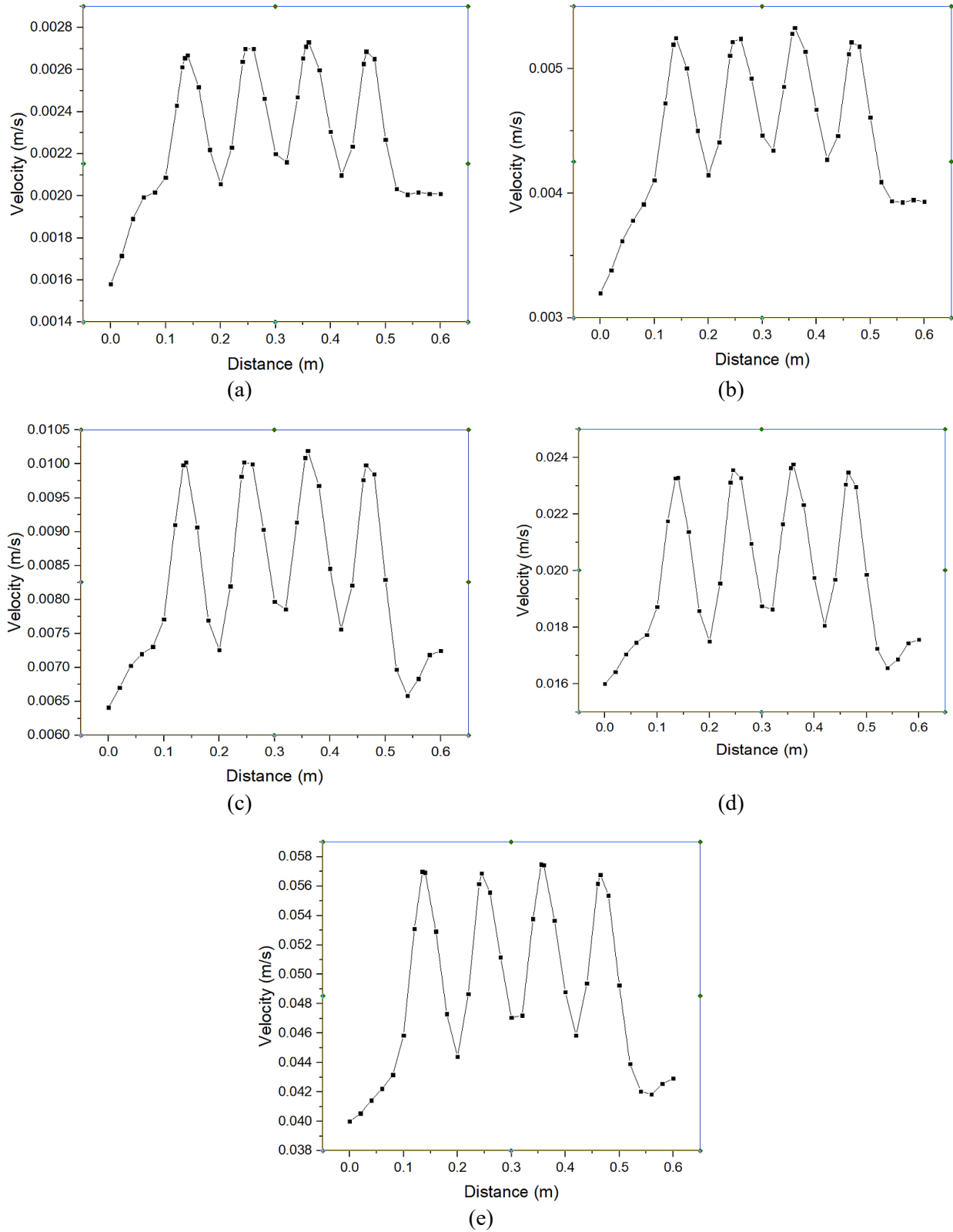


Fig. 10. Effect of fluid flow on velocity Multi-restriction (a) $Re=100$ (b) $Re=200$ (c) $Re=400$ (d) $Re=1000$ (e) $Re=2500$.

6. Conclusion

Through the analysis it was found that, the non-linear pressure drop occurs at the entrance and then at the restriction site. This is because of the increase in velocity and reduction in the flow area of fluid. After repetitive analysis, some values were selected for operating parameters to reduce the effect of restriction and increase heat transfer. This was attained at high turbulence of fluid. The pressure drop at restriction also decreased in a turbulent flow. This restriction in flow caused flow separation and swirl which enhanced the heat transfer and raise the temperature of outlet fluid. Further research is to be done for the optimization of various parameters to increase desired values and decrease others.

Nomenclature

CFD	Computational fluid dynamics
CAD	Computer Aided Design
APV	Agrophotovoltaics
DPD	Dissipative particle dynamics

References

- [1] Tshehla MS, Myers TG, Charpin JPF. The flow of power law fluids between parallel plates with shear heating. *WIT Trans Eng Sci* 2006;52.
- [2] Orszag SA, Kells LC. Transition to turbulence in plane Poiseuille and plane Couette flow. *J Fluid Mech* 1980;96:159. doi:10.1017/S0022112080002066.
- [3] Sundén B, Sköldheden T. Heat transfer and pressure drop in a new type of corrugated channels. *Int Commun Heat Mass Transf* 1985;12:559–66. doi:10.1016/0735-1933(85)90079-X.
- [4] Sunden B, Trollheden S. Periodic laminar flow and heat transfer in a corrugated two-dimensional channel. *Int Commun Heat Mass Transf* 1989;16:215–25. doi:10.1016/0735-1933(89)90023-7.
- [5] Sawyers DR, Sen M, Chang H-C. Heat transfer enhancement in three-dimensional corrugated channel flow. *Int J Heat Mass Transf* 1998;41:3559–73. doi:10.1016/S0017-9310(98)00029-5.
- [6] Béreiziat D, Devienne R. Experimental characterization of Newtonian and non-Newtonian fluid flows in corrugated channels. *Int J Eng Sci* 1999;37:1461–79. doi:10.1016/S0020-7225(98)00126-8.
- [7] Fabbri G. Heat transfer optimization in corrugated wall channels. *Int J Heat Mass Transf* 2000;43:4299–310. doi:10.1016/S0017-9310(00)00054-5.
- [8] Fabbri G, Rossi R. Analysis of the heat transfer in the entrance region of optimised corrugated wall channel. *Int Commun Heat Mass Transf* 2005;32:902–12. doi:10.1016/j.icheatmasstransfer.2004.08.027.
- [9] Mehrabian M., Poulter R. Hydrodynamics and thermal characteristics of corrugated channels: computational approach. *Appl Math Model* 2000;24:343–64. doi:10.1016/S0307-904X(99)00039-6.
- [10] Gradeck M, Hoareau B, Lebouché M. Local analysis of heat transfer inside corrugated channel. *Int J Heat Mass Transf* 2005;48:1909–15. doi:10.1016/j.ijheatmasstransfer.2004.12.026.

- [11] Zimmerer C, Gschwind P, Gaiser G, Kottke V. Comparison of heat and mass transfer in different heat exchanger geometries with corrugated walls. *Exp Therm Fluid Sci* 2002;26:269–73. doi:10.1016/S0894-1777(02)00136-X.
- [12] Wang C-C, Chen C-K. Forced convection in a wavy-wall channel. *Int J Heat Mass Transf* 2002;45:2587–95. doi:10.1016/S0017-9310(01)00335-0.
- [13] Ali AHH, Hanaoka Y. Experimental study on laminar flow forced-convection in a channel with upper V-corrugated plate heated by radiation. *Int J Heat Mass Transf* 2002;45:2107–17. doi:10.1016/S0017-9310(01)00309-X.
- [14] Metwally HM, Manglik RM. Enhanced heat transfer due to curvature-induced lateral vortices in laminar flows in sinusoidal corrugated-plate channels. *Int J Heat Mass Transf* 2004;47:2283–92. doi:10.1016/j.ijheatmasstransfer.2003.11.019.
- [15] Islamoglu Y, Parmaksizoglu C. The effect of channel height on the enhanced heat transfer characteristics in a corrugated heat exchanger channel. *Appl Therm Eng* 2003;23:979–87. doi:10.1016/S1359-4311(03)00029-2.
- [16] Islamoglu Y, Kurt A. Heat transfer analysis using ANNs with experimental data for air flowing in corrugated channels. *Int J Heat Mass Transf* 2004;47:1361–5. doi:10.1016/j.ijheatmasstransfer.2003.07.031.
- [17] Islamoglu Y, Parmaksizoglu C. Numerical investigation of convective heat transfer and pressure drop in a corrugated heat exchanger channel. *Appl Therm Eng* 2004;24:141–7. doi:10.1016/j.applthermaleng.2003.07.004.
- [18] Naphon P. Laminar convective heat transfer and pressure drop in the corrugated channels. *Int Commun Heat Mass Transf* 2007;34:62–71. doi:10.1016/j.icheatmasstransfer.2006.09.003.
- [19] Naphon P. Heat transfer characteristics and pressure drop in channel with V corrugated upper and lower plates. *Energy Convers Manag* 2007;48:1516–24. doi:10.1016/j.enconman.2006.11.020.
- [20] Naphon P. Effect of corrugated plates in an in-phase arrangement on the heat transfer and flow developments. *Int J Heat Mass Transf* 2008;51:3963–71. doi:10.1016/j.ijheatmasstransfer.2007.11.050.
- [21] Tiwari AK, Ghosh P, Sarkar J, Dahiya H, Parekh J. Numerical investigation of heat transfer and fluid flow in plate heat exchanger using nanofluids. *Int J Therm Sci* 2014;85:93–103. doi:10.1016/j.ijthermalsci.2014.06.015.
- [22] Shetab Bushehri MR, Ramin H, Salimpour MR. A new coupling method for slip-flow and conjugate heat transfer in a parallel plate micro heat sink. *Int J Therm Sci* 2015;89:174–84. doi:10.1016/j.ijthermalsci.2014.10.018.
- [23] Rios-Iribe EY, Cervantes-Gaxiola ME, Rubio-Castro E, Ponce-Ortega JM, González-Llanes MD, Reyes-Moreno C, et al. Heat transfer analysis of a non-Newtonian fluid flowing through a circular tube with twisted tape inserts. *Appl Therm Eng* 2015;84:225–36. doi:10.1016/j.applthermaleng.2015.03.052.
- [24] Yang H, Wen J, Gu X, Liu Y, Wang S, Cai W, et al. A mathematical model for flow maldistribution study in a parallel plate-fin heat exchanger. *Appl Therm Eng* 2017;121:462–72. doi:10.1016/j.applthermaleng.2017.03.130.
- [25] Sathish T, Mohanavel V. IWF based optimization of porous insert configurations for heat transfer enhancement using CFD. *J Appl Fluid Mech* 2018;11:31–7.
- [26] Borhani M, Yaghoubi S. Numerical simulation of heat transfer in a parallel plate channel and promote dissipative particle dynamics method using different weight functions. *Int Commun Heat Mass Transf* 2020;115:104606. doi:10.1016/j.icheatmasstransfer.2020.104606.
- [27] Temam R. Navier-Stokes equations: theory and numerical analysis. vol. 343. American Mathematical Soc.; 2001.